Supporting information for:

Ion Transport Mechanisms in Pectin-containing EC-LiTFSI Electrolytes

Sipra Mohapatra[1], *Hema Teherpuria*[1], *Sapta Sindhu Paul Chowdhury*[1], *Suleman Jalilahmad Ansari*[1], *Prabhat K. Jaiswal*[1], *Roland R. Netz*[2], *and Santosh Mogurampelly*[1,2,*]

[1]Department of Physics, Indian Institute of Technology Jodhpur, Karwar, Rajasthan 342037, India.

[2]Fachbereich Physik, Freie Universität Berlin, 14195 Berlin, Germany.

*Corresponding Author: santosh@iitj.ac.in

Abstract:

The supplementary document contains **(S1)** The visual impression of the simulated systems (**S1.1**) The force field parameters for pectin polymer (Table **ST1:** bonded, non-bonded force field parameters for pectin polymer) (Table **ST2:** System details) **(S2)** Radial distribution function and coordination number **(S3)** Ion association probability **(S4)** Mean squared displacement (Table **ST3:** Diffusion coefficient calculations from MSD curves), **(S5**) Calculation of viscosity and notes on numerical issues, **(S6)** Diffusion coefficient scaling with η and τ_c, **(S7)** The ion-pair correlation function, (**S8)** Pectin loading dependency of $\sigma_{NE}, \eta, P(0), P(1)$ and $P(2)$ and an intuitive objective function $f\left(\sigma_{NE}, P(0), P(1)\right) \sim \sigma_{NE} P^a(0) / P^b(1)$, and **(S9)** Transference number with wt. % of pectin.

S1: The Visual Impression of the Simulated Systems:

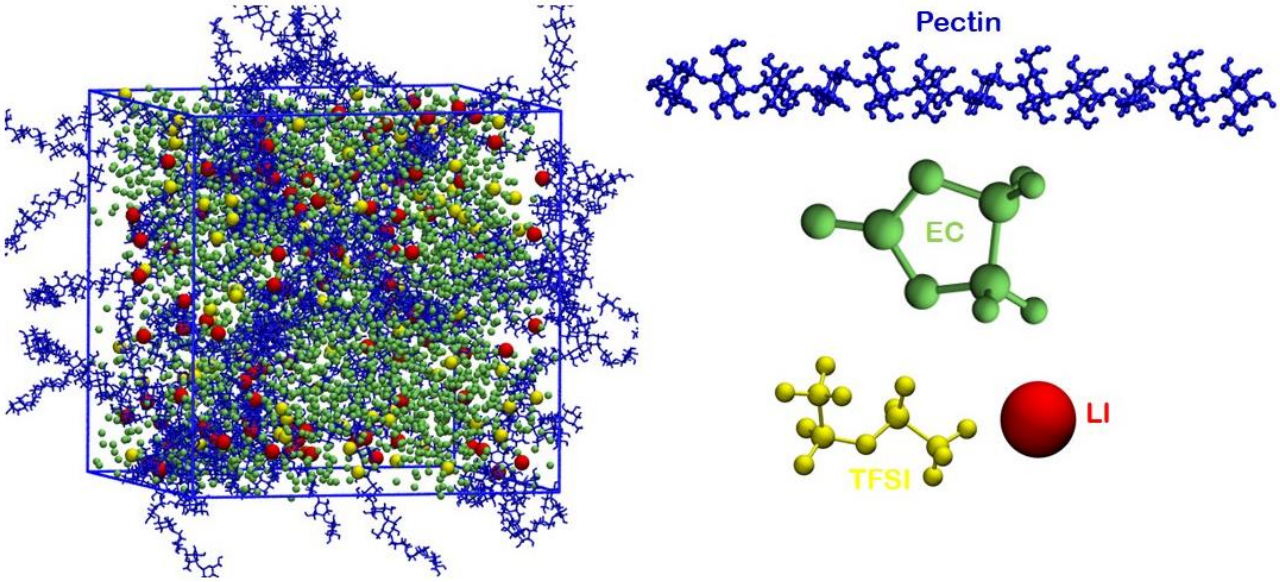

Figure S1: Equilibrated snapshot (collected at 300 ns and 425 K) of the pectin-EC-LiTFSI electrolyte system at a loading of pectin 10 wt. % generated with VMD visualization tool.[1]

S1.1. The Force Field Parameters for Pectin Polymer

The non-bonded parameters are taken directly from GLYCAM06J force field parameter set.[2]

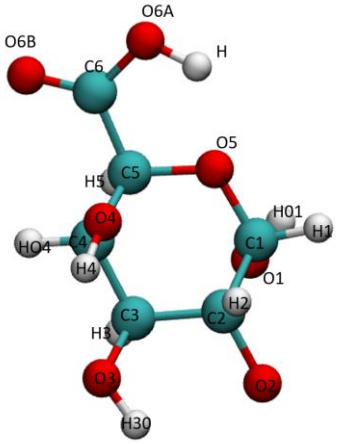

Table ST1: Bonded, Non-bonded Force Field Parameters for Pectin Polymer

Atom type	σ (nm)	ϵ (kJ mol^{-1})	Ref.	q (e)	Ref.
C1	0.339	0.458	GLYCAM06J[2]	0.074	This work
C2	0.339	0.458	GLYCAM06J[2]	0.299	This work
C3	0.339	0.458	GLYCAM06J[2]	0.033	This work
C4	0.339	0.458	GLYCAM06J[2]	0.324	This work
C5	0.339	0.458	GLYCAM06J[2]	-0.385	This work
C6	0.339	0.458	GLYCAM06J[2]	0.849	This work
H1	0.229	0.066	GLYCAM06J[2]	0.116	This work
H1O	0.035	0.126	GLYCAM06J[2]	0.376	This work
H2	0.247	0.066	GLYCAM06J[2]	0.087	This work
H2O	0.035	0.126	GLYCAM06J[2]	0.389	This work
H3	0.247	0.066	GLYCAM06J[2]	0.099	This work
H3O	0.035	0.126	GLYCAM06J[2]	0.409	This work
H4	0.247	0.066	GLYCAM06J[2]	0.063	This work
H4O	0.035	0.126	GLYCAM06J[2]	0.404	This work
H5	0.247	0.066	GLYCAM06J[2]	0.175	This work
HO1	0.035	0.126	GLYCAM06J[2]	0.434	This work
O1	0.306	0.88	GLYCAM06J[2]	-0.581	This work
O2	0.3	0.711	GLYCAM06J[2]	-0.617	This work
O3	0.3	0.711	GLYCAM06J[2]	-0.615	This work
O4	0.3	0.711	GLYCAM06J[2]	-0.339	This work
O5	0.3	0.711	GLYCAM06J[2]	-0.257	This work
O6A	0.3	0.711	GLYCAM06J[2]	-0.535	This work
O6B	0.3	0.711	GLYCAM06J[2]	-0.545	This work

Bond Types	Ref: gromacs_manual_5.0.4 page number 138, table 5.5				
i	**j**	**function**	**b_0 (nm);**	**k_b (kJ mol^{-1} nm^{-2})**	**Ref.**
HO1	O1	1	0.097	196086.09	This work
O1	C1	1	0.142	118925.01	This work

C1	C2	1	0.153	117690.1	This work
C1	H1	1	0.110	125620.67	This work
C1	O5	1	0.142	112750.06	This work
C2	O2	1	0.142	126537.38	This work
C2	H2	1	0.110	128339.14	This work
C2	C3	1	0.153	113959.82	This work
C3	H3	1	0.110	120601.42	This work
C3	O3	1	0.143	124864.28	This work
C3	C4	1	0.153	115552.62	This work
C4	H4	1	0.110	122602.08	This work
C4	C5	1	0.153	110645.46	This work
C4	O4	1	0.142	127070.3	This work
C5	H5	1	0.110	125281.26	This work
C5	O5	1	0.144	111768.7	This work
C5	C6	1	0.153	102048.09	This work
C6	O6A	1	0.134	154705.91	This work
C6	O6B	1	0.121	321628.31	This work
O6A	H1O	1	0.097	183897.09	This work
O4	H4O	1	0.097	193553.97	This work
O3	H3O	1	0.097	193097.12	This work
O2	H2O	1	0.097	191439.8	This work
O4	C1	1	0.139	149781.22	This work

Angle Types	Ref: gromacs_manual_5.0.4 page number 138, table 5.5							
i	**j**	**k**	**function**	**θ_0 (deg)**	**k_θ (kJ mol^{-1} rad^{-2})**	**r_{13} (nm)**	**k_{UB} (kJ mol^{-1} nm^{-2})**	**Ref.**
HO1	O1	C1	5	109.347	180.639	0	0	This work
O1	C1	C2	5	106.898	450.234	0	0	This work
H1	C1	C2	5	110.811	237.645	0	0	This work
C2	C1	O5	5	111.427	1124.423	0	0	This work
O1	C1	H1	5	110.821	269.745	0	0	This work
O1	C1	O5	5	112.148	471.801	0	0	This work

H1	C1	O5	5	104.810	269.463	0	0	This work
C1	C2	O2	5	111.669	380.449	0	0	This work
C1	C2	H2	5	107.975	239.426	0	0	This work
C1	C2	C3	5	111.002	1255.179	0	0	This work
H2	C2	O2	5	106.156	264.376	0	0	This work
C3	C2	O2	5	111.26	372.586	0	0	This work
H2	C2	C3	5	108.557	239.988	0	0	This work
H3	C3	O3	5	110.055	268.286	0	0	This work
C2	C3	H3	5	109.371	238.441	0	0	This work
H3	C3	C4	5	108.692	235.478	0	0	This work
C2	C3	O3	5	110.902	379.229	0	0	This work
C4	C3	O3	5	107.258	388.506	0	0	This work
C2	C3	C4	5	110.519	1255.179	0	0	This work
C3	C4	H4	5	109.644	229.586	0	0	This work
H4	C4	C5	5	107.891	227.911	0	0	This work
H4	C4	O4	5	110.692	267.557	0	0	This work
C3	C4	C5	5	108.947	1255.179	0	0	This work
C3	C4	O4	5	111.278	406.091	0	0	This work
C5	C4	O4	5	108.302	396.739	0	0	This work
H5	C5	O5	5	109.764	278.376	0	0	This work
H5	C5	C6	5	106.897	209.052	0	0	This work
C4	C5	H5	5	108.671	235.004	0	0	This work
C6	C5	O5	5	108.353	459.009	0	0	This work
C4	C5	O5	5	112.098	1115.862	0	0	This work
C4	C5	C6	5	110.923	327.898	0	0	This work
C5	C6	O6A	5	116.12	446.296	0	0	This work
C5	C6	O6B	5	121.273	383.507	0	0	This work
O6A	C6	O6B	5	122.604	438.97	0	0	This work
C6	O6A	H1O	5	108.239	211.453	0	0	This work
C1	O5	C5	5	115.565	841.824	0	0	This work
C4	O4	H4O	5	107.212	193.249	0	0	This work
C3	O3	H3O	5	107.778	188.268	0	0	This work

C2	O2	H2O	5	107.517	196.578	0	0	This work
O4	C1	C2	5	111.915	480.242	0	0	This work
O4	C1	H1	5	108.716	269.634	0	0	This work
O4	C1	O5	5	117.376	455.385	0	0	This work
C4	O4	C1	5	113.244	584.861	0	0	This work

Dihedral types	Ref: gromacs_manual_5.0.4 page number 139, table 5.5							
i	**j**	**k**	**l**	**function**	**φ_s (Deg)**	**k_φ (kJ mol^{-1})**	**Multiplicity**	**Ref.**
HO1	O1	C1	C2	9	0	0.753	3	GLYCAM06J[2]
HO1	O1	C1	H1	9	0	0.753	3	GLYCAM06J[2]
HO1	O1	C1	O5	9	0	0.753	3	GLYCAM06J[2]
O1	C1	C2	O2	9	0	-0.418	1	GLYCAM06J[2]
O1	C1	C2	H2	9	0	0.209	3	GLYCAM06J[2]
O1	C1	C2	C3	9	0	0.418	3	GLYCAM06J[2]
H1	C1	C2	O2	9	0	0.209	3	GLYCAM06J[2]
H1	C1	C2	H2	9	0	0.711	3	GLYCAM06J[2]
H1	C1	C2	C3	9	0	0.628	3	GLYCAM06J[2]
O5	C1	C2	O2	9	0	-4.602	1	GLYCAM06J[2]
O5	C1	C2	H2	9	0	0.209	3	GLYCAM06J[2]
O5	C1	C2	C3	9	0	-1.130	1	GLYCAM06J[2]
C2	C1	O5	C5	9	0	0.669	3	GLYCAM06J[2]
O1	C1	O5	C5	9	0	4.017	3	GLYCAM06J[2]
H1	C1	O5	C5	9	0	0.418	3	GLYCAM06J[2]
C1	C2	O2	H2O	9	0	0.753	3	GLYCAM06J[2]
H2	C2	O2	H2O	9	0	0.753	3	GLYCAM06J[2]
C3	C2	O2	H2O	9	0	0.753	3	GLYCAM06J[2]
C1	C2	C3	H3	9	0	0.628	3	GLYCAM06J[2]
C1	C2	C3	O3	9	0	0.418	3	GLYCAM06J[2]
C1	C2	C3	C4	9	0	1.883	1	GLYCAM06J[2]
O2	C2	C3	H3	9	0	0.209	3	GLYCAM06J[2]
O2	C2	C3	O3	9	0	-0.418	1	GLYCAM06J[2]
O2	C2	C3	C4	9	0	0.418	3	GLYCAM06J[2]
H2	C2	C3	H3	9	0	0.711	3	GLYCAM06J[2]

H2	C2	C3	O3	9	0	0.209	3	GLYCAM06J[2]
H2	C2	C3	C4	9	0	0.628	3	GLYCAM06J[2]
H3	C3	O3	H3O	9	0	0.753	3	GLYCAM06J[2]
C2	C3	O3	H3O	9	0	0.753	3	GLYCAM06J[2]
C4	C3	O3	H3O	9	0	0.753	3	GLYCAM06J[2]
H3	C3	C4	H4	9	0	0.711	3	GLYCAM06J[2]
H3	C3	C4	C5	9	0	0.628	3	GLYCAM06J[2]
H3	C3	C4	O4	9	0	0.209	3	GLYCAM06J[2]
O3	C3	C4	H4	9	0	0.209	3	GLYCAM06J[2]
O3	C3	C4	C5	9	0	0.418	3	GLYCAM06J[2]
O3	C3	C4	O4	9	0	1.046	2	GLYCAM06J[2]
C2	C3	C4	H4	9	0	0.628	3	GLYCAM06J[2]
C2	C3	C4	C5	9	0	1.883	1	GLYCAM06J[2]
C2	C3	C4	O4	9	0	-1.13	1	GLYCAM06J[2]
H4	C4	C5	H5	9	0	0.711	3	GLYCAM06J[2]
H4	C4	C5	O5	9	0	0.209	3	GLYCAM06J[2]
H4	C4	C5	C6	9	0	0.418	3	GLYCAM06J[2]
C3	C4	C5	H5	9	0	0.628	3	GLYCAM06J[2]
C3	C4	C5	O5	9	0	-1.13	1	GLYCAM06J[2]
C3	C4	C5	C6	9	0	1.883	1	GLYCAM06J[2]
O4	C4	C5	H5	9	0	0.209	3	GLYCAM06J[2]
O4	C4	C5	O5	9	0	1.674	2	GLYCAM06J[2]
O4	C4	C5	C6	9	0	0.418	2	GLYCAM06J[2]
H4	C4	O4	H4O	9	0	0.753	3	GLYCAM06J[2]
C3	C4	O4	H4O	9	0	0.753	3	GLYCAM06J[2]
C5	C4	O4	H4O	9	0	0.753	3	GLYCAM06J[2]
H5	C5	O5	C1	9	0	1.13	3	GLYCAM06J[2]
C6	C5	O5	C1	9	0	1.339	3	GLYCAM06J[2]
C4	C5	O5	C1	9	0	0.669	3	GLYCAM06J[2]
H5	C5	C6	O6A	9	0	0	1	GLYCAM06J[2]
H5	C5	C6	O6B	9	0	0	1	GLYCAM06J[2]
O5	C5	C6	O6A	9	0	0.084	1	GLYCAM06J[2]
O5	C5	C6	O6B	9	0	0.084	1	GLYCAM06J[2]

C4	C5	C6	O6A	9	0	0.021	1	GLYCAM06J[2]
C4	C5	C6	O6B	9	0	0.021	1	GLYCAM06J[2]
C5	C6	O6A	H1O	9	0	0.753	3	GLYCAM06J[2]
O6B	C6	O6A	H1O	9	0	0.753	3	GLYCAM06J[2]
C3	C4	O4	C1	9	0	0.669	3	GLYCAM06J[2]
C5	C4	O4	C1	9	0	0.669	3	GLYCAM06J[2]
H4	C4	O4	C1	9	0	1.13	3	GLYCAM06J[2]
C4	O4	C1	H1	9	0	0.418	3	GLYCAM06J[2]
C4	O4	C1	C2	9	0	0.669	3	GLYCAM06J[2]
C4	O4	C1	O5	9	0	4.017	3	GLYCAM06J[2]
O4	C1	C2	C3	9	0	-1.13	1	GLYCAM06J[2]
O4	C1	C2	H2	9	0	0.209	3	GLYCAM06J[2]
O4	C1	C2	O2	9	0	1.046	2	GLYCAM06J[2]
O4	C1	O5	C5	9	0	4.017	3	GLYCAM06J[2]

Table ST2: System Compositional Details

Pectin wt. %	No. of EC molecules	No. of pectin chains	No. of Li	No. of TFSI	Total No. of Atoms
50	2420	100	100	100	53300
30	3388	60	100	100	53580
10	4356	20	100	100	53860
5	4598	10	100	100	53930
3	4695	6	100	100	53960
2	4743	4	100	100	53970
1	4791	2	100	100	53990
0.5	4816	1	100	100	53995
0	4840	0	100	100	54000

S2: Radial Distribution Functions and Coordination Numbers

The structural properties of the electrolytes were studied by calculating the radial distribution function g(r) and coordination number CN(r) of anion and cation. Further, to investigate the interaction between the ion-ion and ion-polymer, we have calculated the RDF and CN(r) for different pairs such as Li-N_{TFSI} , O_{EC}-Li, O_{EC}-N_{TFSI}, O_{pectin}-Li, O_{pectin}-N_{TFSI}, O_{pectin}-O_{EC}, etc.

We found sharp peaks in RDF for Li-O (pectin), Li-TFSI, and Li- (O)EC and broadened peaks for other pairs showing the strong interaction between lithium and oxygen units of other molecules. The coordination number supports the RDF results. To get a better idea, we have also calculated the ion association probability of the ions.

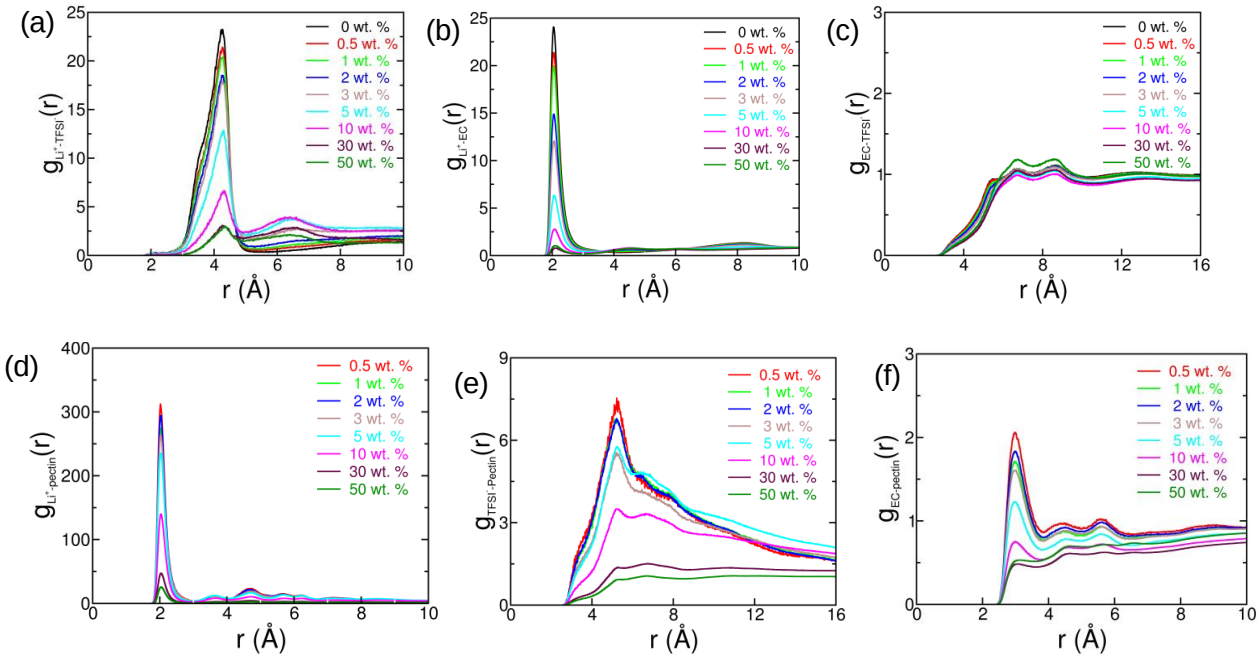

Figure S2.1: Radial distribution function and CN(r) for different atomic pairs such as Li-N_{TFSI} , Li-O_{EC}, O_{EC}-N_{TFSI} , Li-O_{pectin}, N_{TFSI} -O_{pectin}, O_{pectin}-O_{EC}.

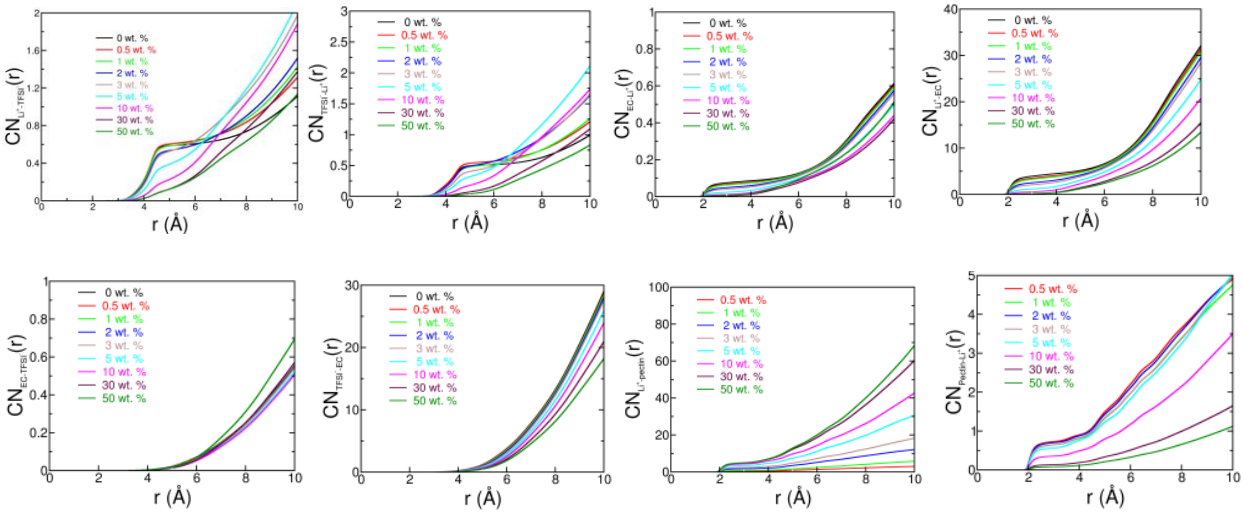

Figure S2.2: Coordination number of atomic pairs of Li, TFSI, EC molecule at different loadings of pectin.

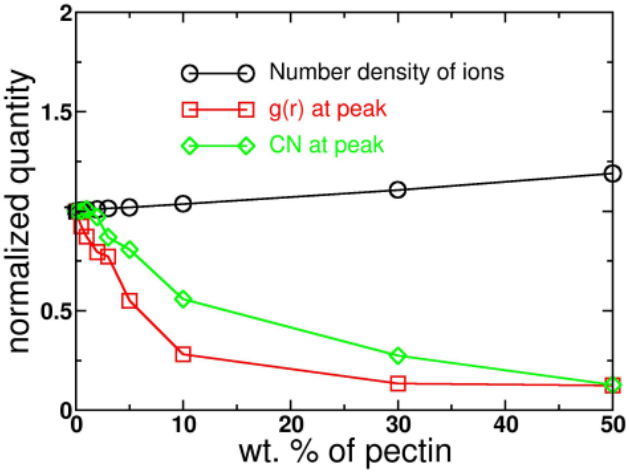

Figure S2.3: The normalized number density of ions, g(r) at first peak and CN(r) at first peak corresponding to the pairs Li-TFSI.

S3: Ion-Association Probability

The P(n) is calculated using the formula $P(n) = \frac{1}{N_{\text{frames}}} \sum_{i=1}^{N_{\text{frames}}} \sum_{j=1}^{N_{\text{ions}}} \frac{\delta_{n_i n_j}}{N_{\text{ions}}}$, where $\delta_{n_i n_j}$ is the Kronecker delta function to count n number of counterions within the first coordination shell of the ion j, N_{ions} is the total number of ions, N_{frames} is the total number of frames. Here, $\delta_{n_i n_j}$ is defined in such a way that $\delta_{n_i n_j} = 1$ if n_i^{th} ion is found within the first coordination shell of n_j^{th} ion, and $\delta_{n_i n_j} = 0$, otherwise.

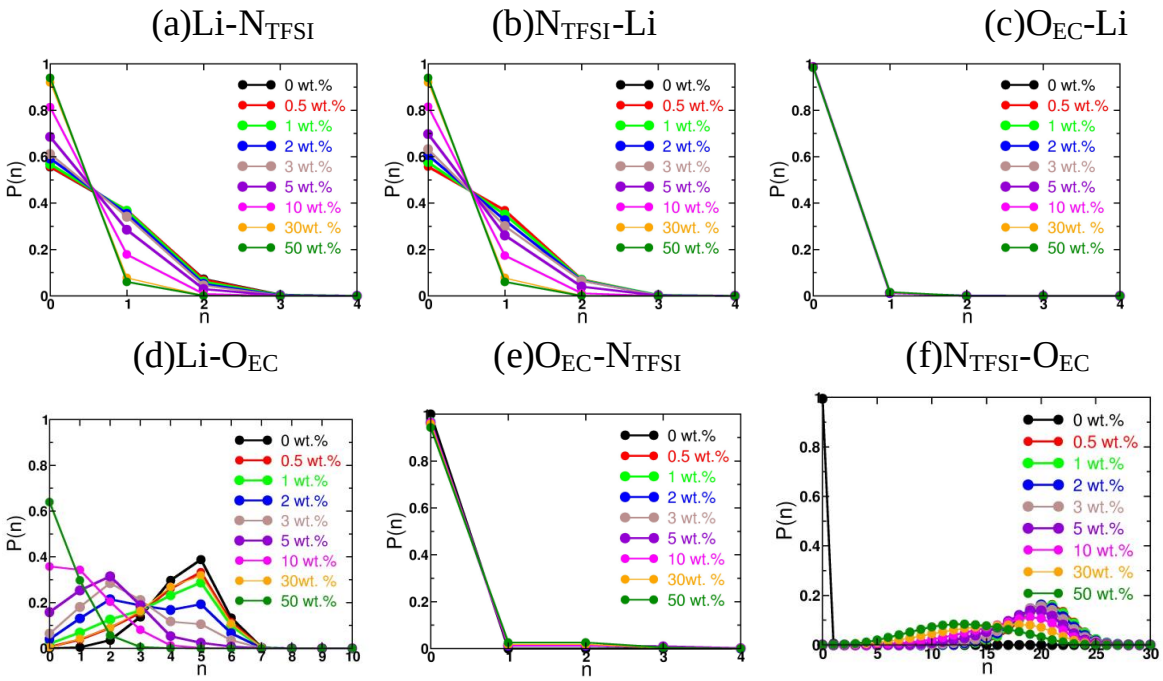

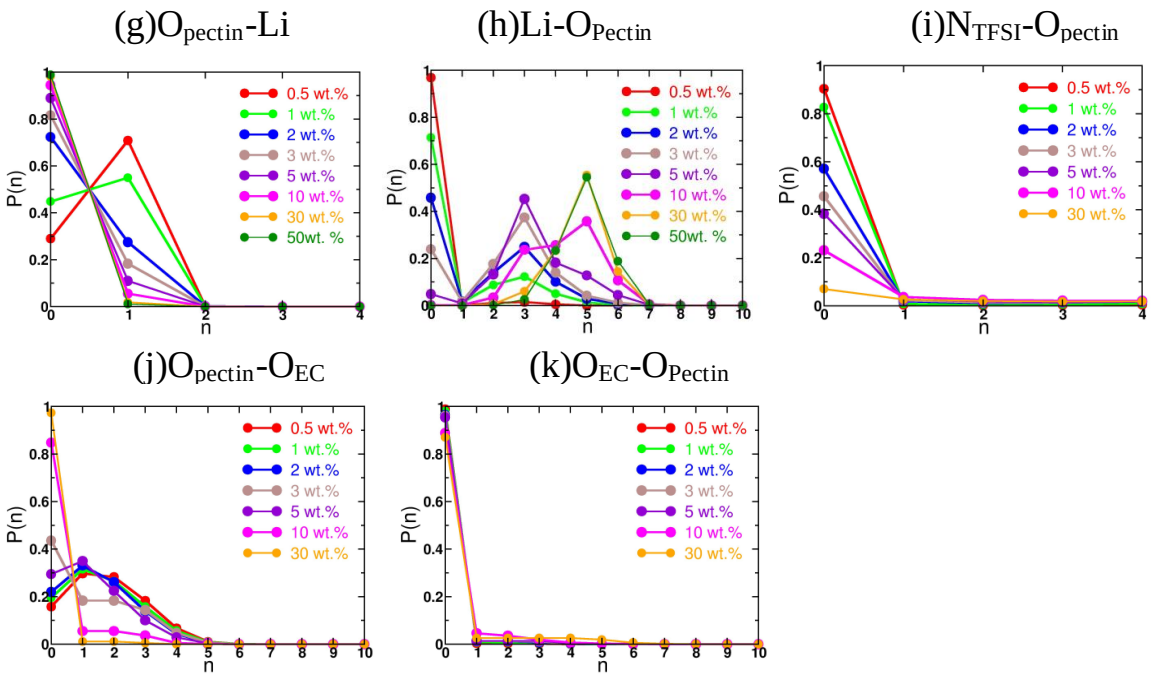

Figure S3: Probability of $TFSI^-$ around Li^+ ions for different atomic pairs such as Li-N_{TFSI} , Li-O_{EC}, Li-O_{pectin}, N_{TFSI} -O_{pectin}, O_{EC}-N_{TFSI} , O_{pectin}-O_{EC} etc.

S4: Mean Squared Displacements

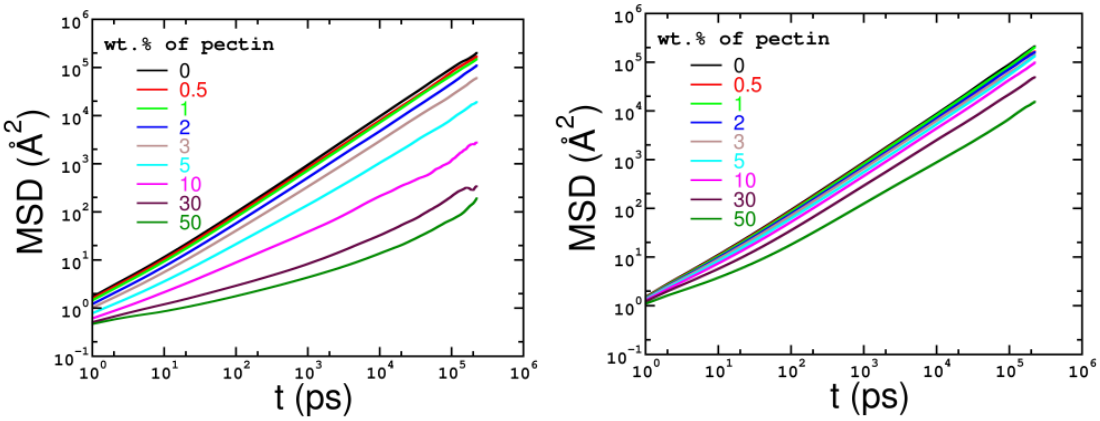

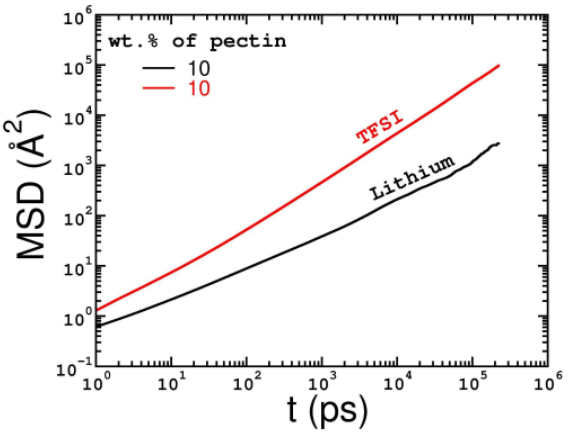

Figure S4: Mean square displacement of (a) Li^+ (b) $TFSI^-$ for all wt.%, and (c) comparison of both Li^+ and $TFSI^-$

Table ST3: Diffusion Coefficient Calculations from MSD curves

wt. % of pectin	Exponent λ in MSD$(t)\sim t^{\lambda}$	Range used for fitting	MSD (slope) ($Å^2/s$)	D_{Li} (cm^2/s)
0	1.04	(179-223) ns	0.95	1.58E-05
0.5	0.94	(97-162) ns	0.85	1.41E-05
1	1.04	(190-223) ns	0.66	1.10E-05
2	1.07	(186-222) ns	0.48	7.97E-06
3	0.94	(188-222) ns	0.27	4.49E-06
5	1.10	(137-198) ns	0.092	1.53E-06
10	1.06	(122-181) ns	0.01	2.17E-07
30	1.02	(85-140) ns	0.002	3.54E-08
50	0.96	(101-158) ns	0.0005	9.40E-09

wt. % of pectin	Exponent λ in MSD$(t)\sim t^{\lambda}$	Range used for fitting	MSD (slope) ($Å^2/s$)	D_{TFSI} (cm^2/s)

0	1.06	(168-220) ns	0.92	1.53E-05
0.5	0.94	(145-200) ns	0.77	1.28E-05
1	1.01	(133-193) ns	0.83	1.38E-05
2	0.99	(141-210) ns	0.72	1.20E-05
3	1.10	(152-216) ns	0.61	1.02E-05
5	1.10	(194-224) ns	0.53	8.85E-06
10	1.06	(179-222) ns	0.43	7.21E-06
30	1.00	(174-223) ns	0.22	3.65E-06
50	0.87	(167-221) ns	0.07	1.15E-06

S5: Calculation of Viscosity and Notes on Numerical Issues

It is often desirable to compute the time autocorrelation functions (TACFs) by picking the lag-time logarithmically for computational efficiency-related code optimizations. However, when using such time autocorrelation functions in the integration, it is possible to overlook the numerical errors. In **Figure S5**, we show a typical normalized TACF, $\langle P_{\alpha\beta}(t)P_{\alpha\beta}(0)\rangle / \langle P_{\alpha\beta}(0)P_{\alpha\beta}(0)\rangle$, and its numerically obtained running integral of viscosity, $\eta = \frac{V}{k_B T}\frac{1}{6}\sum_{\alpha\beta}\int_0^\infty d\tau \langle P_{\alpha\beta}(t)P_{\alpha\beta}(0)\rangle$ with different choices in picking the lagtimes and the number of data points in TACF. The results indicate that while a higher number of data points in TACF produce fewer errors when the lag-times are picked logarithmically, straightforward integration of TACF with linearly picked lag-times produces minimal errors in the calculation of η. Part of the Fortran code to calculate η is given below, for an interested reader, and the full code is available upon request. However, choosing longer trajectories and a large set of independent trajectories reduces further errors in η. In this paper, we chose 50 uncorrelated independent trajectories for sampling the η calculations.

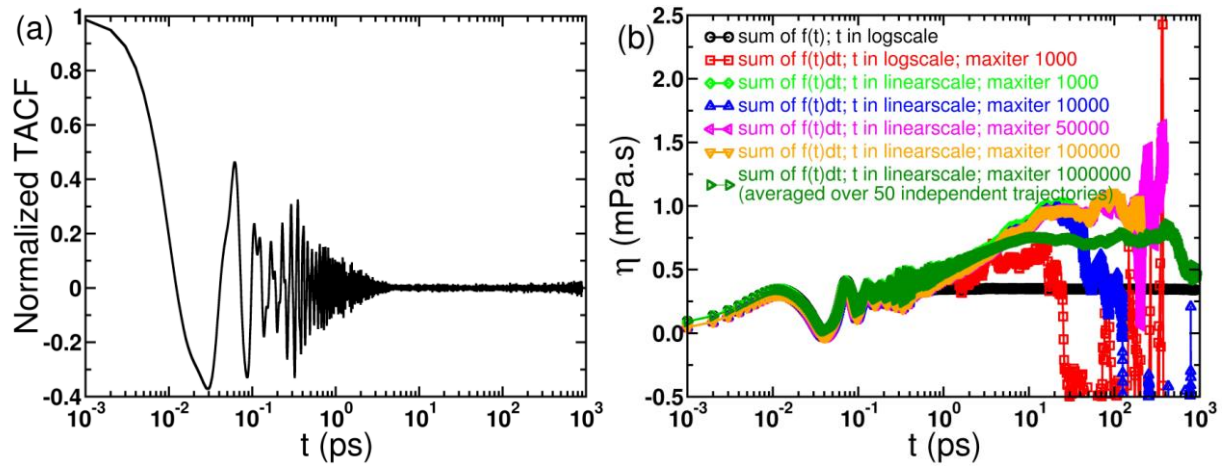

Figure S5: (a) Normalized time autocorrelation function, and (b) its numerical integration for pectin-EC-LiTFSI electrolytes at 0 wt. % of the pectin loading.

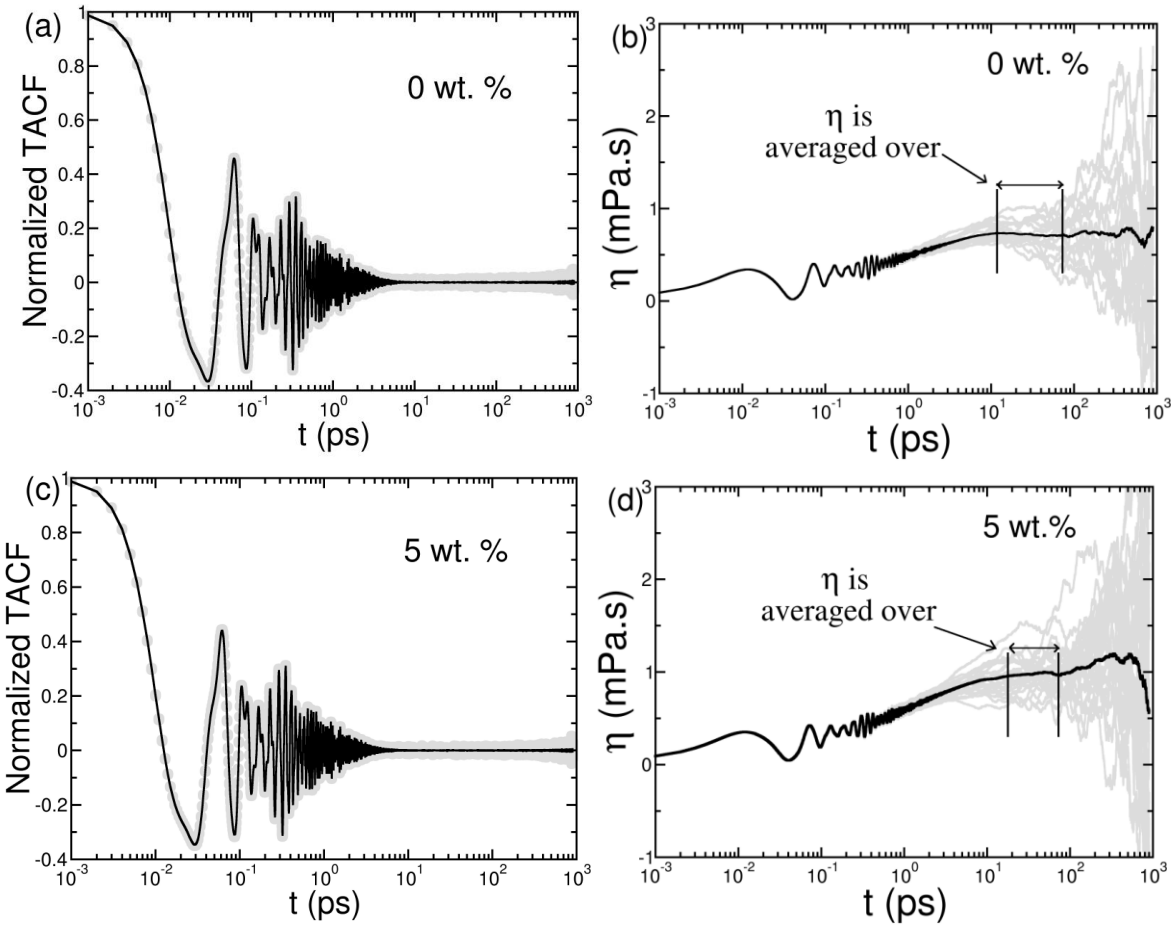

Figure S6: (a), (c) Average time autocorrelation function for 0 wt. % and 5 wt. % pectin loading and (b), (d) corresponding running integral from 50 independent trajectories.

Fortran95 Code [full version is available on request]:

```
!calculating viscosity
 pxyacf=0.0d0
 pxzacf=0.0d0
 pyzacf=0.0d0
 pyxacf=0.0d0
 pzxacf=0.0d0
 pzyacf=0.0d0
 etaavg=0.0d0
 etapxy=0.0d0
 etapxz=0.0d0
 etapyz=0.0d0
 etapyx=0.0d0
 etapzx=0.0d0
 etapzy=0.0d0
 r1=0.0d0
 i1=0
 tau=1
 maxiter=min(10000,taumax)
 do itau=1,maxiter
 !do tau=1,taumax
  tauold=tau
  tau=nint(10.0d0**(r1)) !pick tau logarithmically increasing order:
r1=r1+log10(float(taumax))/maxiter
  if(itau.eq.1.or.tau.gt.tauold)then
   i1=i1+1
   do k=1,nframes-tau
    pxyacf(tau)=pxyacf(tau)+pxy(k)*pxy(k+tau-1)
    pxzacf(tau)=pxzacf(tau)+pxz(k)*pxz(k+tau-1)
    pyzacf(tau)=pyzacf(tau)+pyz(k)*pyz(k+tau-1)
    pyxacf(tau)=pyxacf(tau)+pyx(k)*pyx(k+tau-1)
    pzxacf(tau)=pzxacf(tau)+pzx(k)*pzx(k+tau-1)
    pzyacf(tau)=pzyacf(tau)+pzy(k)*pzy(k+tau-1)
   enddo !do k=1,nframes-tau
!normalize distacf
   norm=(nframes-tau) !normalization for individual off-diagonal components of pressure tensor
   pxyacf(tau)=pxyacf(tau)/norm
   pxzacf(tau)=pxzacf(tau)/norm
   pyzacf(tau)=pyzacf(tau)/norm
   pyxacf(tau)=pyxacf(tau)/norm
   pzxacf(tau)=pzxacf(tau)/norm
   pzyacf(tau)=pzyacf(tau)/norm
   pavgacf(tau)=pxyacf(tau)+pxzacf(tau)+pyzacf(tau)+pyxacf(tau)+pzxacf(tau)+pzyacf(tau)
```

```
   pavgacf(tau)=pavgacf(tau)/6.0d0 !normalization for pressure averaged over 6 off-diagonal
components of pressure tensor
  ! write(poftopfid,'(f10.3,7f22.10)')(tau-
1)*timeperframe,pavgacf(tau),pxyacf(tau),pxzacf(tau),pyzacf(tau),pyxacf(tau),&
  !   &pzxacf(tau),pzyacf(tau)
   write(poftopfid,'(f10.3,7f15.10)')(tau-
1)*timeperframe,pavgacf(tau)/pavgacf(1),pxyacf(tau)/pxyacf(1),pxzacf(tau)/pxzacf(1),&
     &pyzacf(tau)/pyzacf(1),pyxacf(tau)/pyxacf(1),pzxacf(tau)/pzxacf(1),pzyacf(tau)/pzyacf(1)
   if(tau.eq.1)then
    write(*,*)
    write(*,*)"pavgacf(1),pxyacf(1),pxzacf(1),pyzacf(1),pyxacf(1),pzxacf(1),pzyacf(1)"
    write(*,'(7f22.10)')pavgacf(1),pxyacf(1),pxzacf(1),pyzacf(1),pyxacf(1),pzxacf(1),pzyacf(1)
    write(*,*)
   endif !if(tau.eq.1)then
   if(tau.eq.1.or.mod(i1,maxiter/10).eq.0)then
    call cpu_time(tf)

write(*,'(a7,2x,i8,2x,a2,2x,i8,2x,a1,1x,F10.2,2x,a26,2x,i8,2x,a7,2x,F10.2,2x,a7)')'POFT:',tau,'of',
nframes,';',&
     &100.0d0*float(tau)/(taumax-1),'% complete; Time taken for',tau,'tau is:',tf-ti,'seconds'
   endif
   dt=tau-tauold
   etaavg=etaavg+volumebykbt*pavgacf(tau)*unitconversion*dt
   etapxy=etapxy+volumebykbt*pxyacf(tau)*unitconversion*dt
   etapxz=etapxz+volumebykbt*pxzacf(tau)*unitconversion*dt
   etapyz=etapyz+volumebykbt*pyzacf(tau)*unitconversion*dt
   etapyx=etapyx+volumebykbt*pyxacf(tau)*unitconversion*dt
   etapzx=etapzx+volumebykbt*pzxacf(tau)*unitconversion*dt
   etapzy=etapzy+volumebykbt*pzyacf(tau)*unitconversion*dt
   write(etaoftopfid,'(f10.3,7f22.10)')(tau-
1)*timeperframe,etaavg,etapxy,etapxz,etapyz,etapyx,etapzx,etapzy
  endif !if(itau.eq.1.or.tau.gt.tauold)then
  r1=r1+log10(float(taumax))/maxiter
 enddo !do itau=1,maxiter
```

S6: Diffusion coefficient scaling with η and τ_C

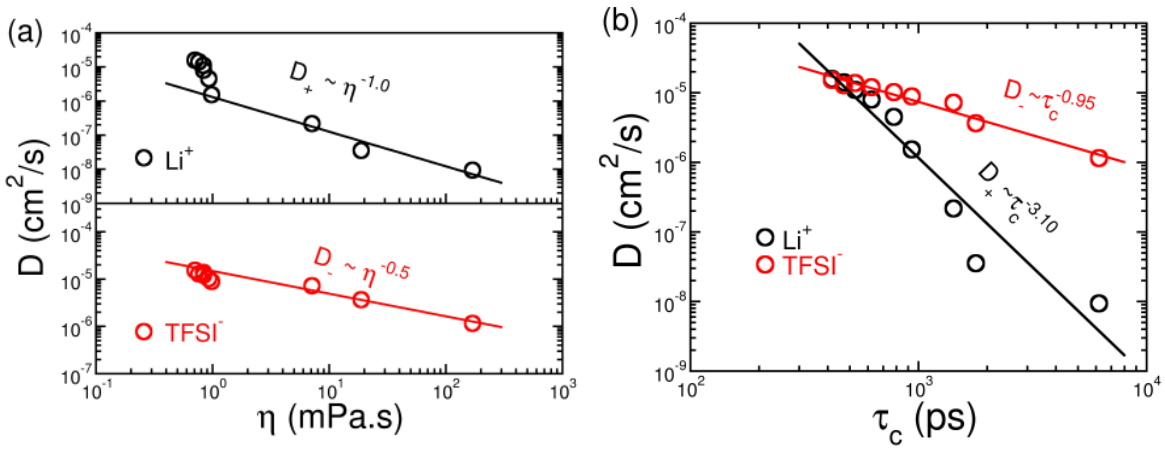

Figure S7: Direct comparison of the diffusion coefficient of Li^+ and $TFSI^-$ ions and their correlations with (a) viscosity and (b) ion-pair relaxation timescales.

In **Figures S7(a)** and **(b)**, we display the diffusivity of ions against the viscosity and ion-pair relaxation timescales, respectively. For the Li^+ and $TFSI^-$ ions, the diffusivity decreases with the viscosity and ion-pair relaxation timescales. Specifically, for the $TFSI^-$ ions, by fitting diffusivities to respective power laws, $D_-\sim\eta^{-\lambda}$ and $D_-\sim\tau_c^{-\lambda}$, we obtain the exponents of 0.5 and 0.95, respectively. Clearly, the $D\sim\eta^{-\lambda}$ relation is violated for $TFSI^-$ ions with viscosities (i.e., $D_-\sim\eta^{-0.5}$) but not with the ion-pair relaxation timescales (i.e., $D_-\sim\tau_c^{-0.95}$). The excellent correlations found between diffusivities of $TFSI^-$ ions and ion-pair relaxation timescales are similar to those reported for traditional liquid electrolytes. However, for the Li^+ ions, a similar analysis shows that $D_+\sim\eta^{-1}$ for higher loadings, obeying the $D\sim\eta^{-\lambda}$ relation with viscosities. On the other hand, the diffusivity of Li^+ ions with the ion-pair relaxations scales as $D_+\sim\tau_c^{-3.1}$, violating the $D\sim\tau_C^{-\lambda}$ relation.

By comparing the diffusivity of ions and viscosity, we found that the diffusivities of $TFSI^-$ ions follow the power law, $D_-\sim\eta^{-0.5}$, revealing the violation of $D\sim\eta^{-\lambda}$ relation with viscosities. Interestingly, the diffusivities of Li^+ ions are observed to obey the $D\sim\eta^{-\lambda}$ relation with viscosities, i.e., $D_+\sim\eta^{-1}$ for higher loadings. Counterintuitively, the ion-pair relaxation timescales revealed opposite trends for the $D\sim\tau_C^{-\lambda}$ relation. Explicitly, while the diffusivities of $TFSI^-$ ions obey the $D\sim\tau_C^{-\lambda}$ relation with ion-pair relaxation timescales (i.e., $D_-\sim\tau_c^{-0.95}$), the diffusivity of Li^+ ions do not obey the $D\sim\tau_C^{-\lambda}$ relation (i.e., $D_+\sim\tau_c^{-3.1}$). The excellent correlations found between diffusivities of $TFSI^-$ ions and ion-pair relaxation timescales are consistent with previous reports. The lithium ion diffusivity does not correlate with ion-pair relaxation time because the polymeric pectin units trap the lithium ions. The Nernst-Einstein conductivity scales with viscosity as $\sigma_{NE}\sim\eta^{-0.56}$ and scales with ion-pair relaxation timescales as $\sigma_{NE}\sim\tau_c^{-1.85}$, revealing distinct transport mechanisms for ionic conductivity.

S7: The Ion-pair Autocorrelation Function

We investigated the structural relaxation phenomena dictated by ion association to understand the transport mechanisms. To quantify the ion-association relaxation phenomena, we computed the ion-pair correlation function $C(t)$, which signifies the relaxation behavior of all ion associations. The ion-pair correlation function $C(t)$ is defined as,

$$C(t) = \frac{\langle h(t)h(0)\rangle}{\langle h(0)h(0)\rangle}$$

The angular bracket $\langle \cdot \cdot \cdot \rangle$ denotes an ensemble average that includes averaging over all ion-pairs and all possible time origins, and $h(t)$ assigned a value unity if lithium and TFSI ions are found within a specified cutoff distance and zero otherwise.

Figure S8.1 (a) shows that the ion-pair relaxation time (τ_C) is highly affected by the loading of pectin. Specifically, we observed that ion-pair relaxation time increases with the increasing wt. % of pectin and, at 10 wt. % of pectin, it becomes almost 10 times higher than the ion-pair relaxation time of neat electrolyte.

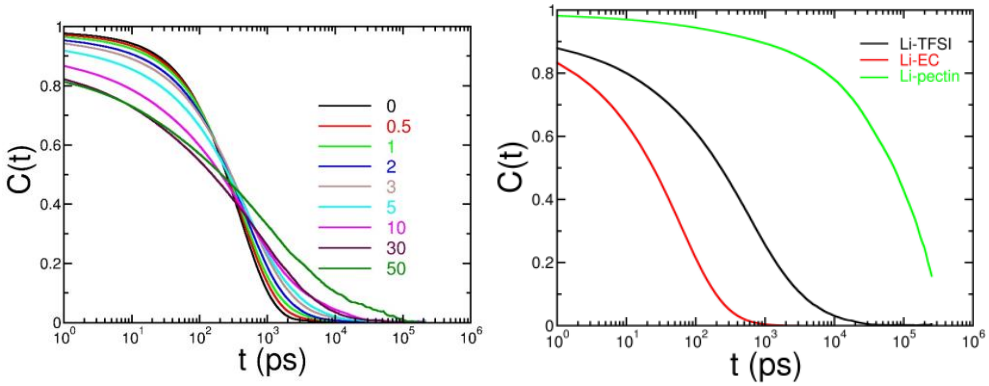

Figure S8.1: The ion-pair correlation function between Li^+ and $TFSI^-$ and (b) comparison of the time correlation function of Li-TFSI with Li-EC and Li-pectin at 10 wt. % of pectin loading.

We calculated the time correlation function and the corresponding relaxation times for atomic pairs between (a) Li and EC and (b) Li and pectin and compared the same with those of Li and TFSI pairs. We chose O04 as representative atom of EC and the most interacting oxygen O2 as the representative atom of pectin for calculating the time correlation functions (see **Figure S8.2**). Still, the number of oxygen atoms of EC and pectin molecules present in our pectin-loaded systems is very high, and hence the computational requirements in computing the time autocorrelation functions are huge due to some factors such as algorithmic complexity, pairwise computations, and memory requirements. Therefore, instead of calculating C(t) for all wt. %s of pectin, we choose only one system (at 10 wt.%) and compare the residence time between the Li-TFSI, Li-EC, and Li-pectin in **Figure S8.1b**. In brief, we observed that the C(t) for lithium-EC decays much faster compared to the C(t) of Li-TFSI pairs. On the other hand, the C(t) for lithium-pectin decays much slower compared to the C(t) of Li-TFSI pairs. Therefore, the relaxation timescales associated with the atomic pairs between (a) Li and EC, (b) Li and TFSI,

and (c) Li and pectin follows the trend: τ_c(Li-EC) < τ_c(Li-TFSI) << τ_c(Li-pectin) and the corresponding numbers are provided in **Table ST4**.

wt. % of pectin	τ_c (Li-EC) in ps	τ_c (Li-TFSI) in ps	τ_c (Li-pectin) in ps
10	78.3	1308.0	190487.8

Table ST4: The relaxation time of Li-TFSI, Li-EC, and Li-pectin at 10 wt. % of pectin loading.

The above analysis clearly demonstrates that the relaxation or residence timescales of the cation near the polymer is very high due to the strong interaction between Li and pectin. Similarly, the relaxation or residence timescales of the cation near the solvent and anion is relatively low due to the respective weaker interactions due to the loading of pectin.

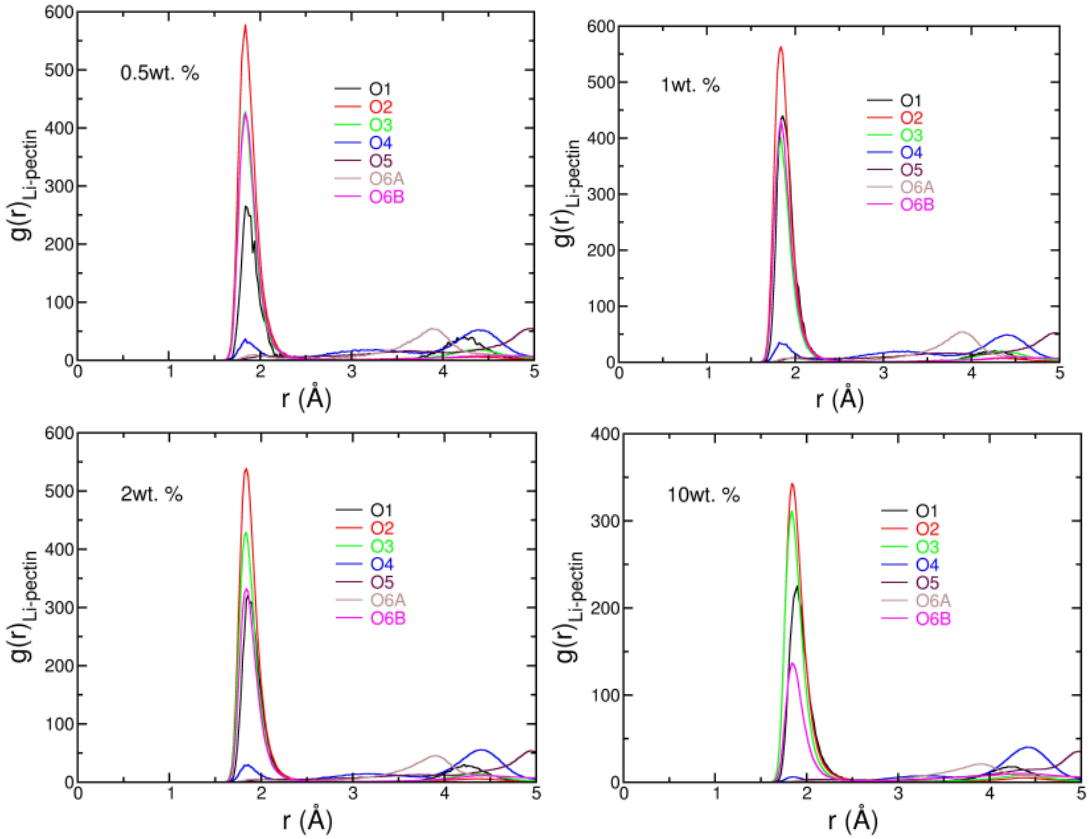

Figure S8.2: The RDF between Li and different oxygen atoms of pectin at different wt. % of pectin loading.

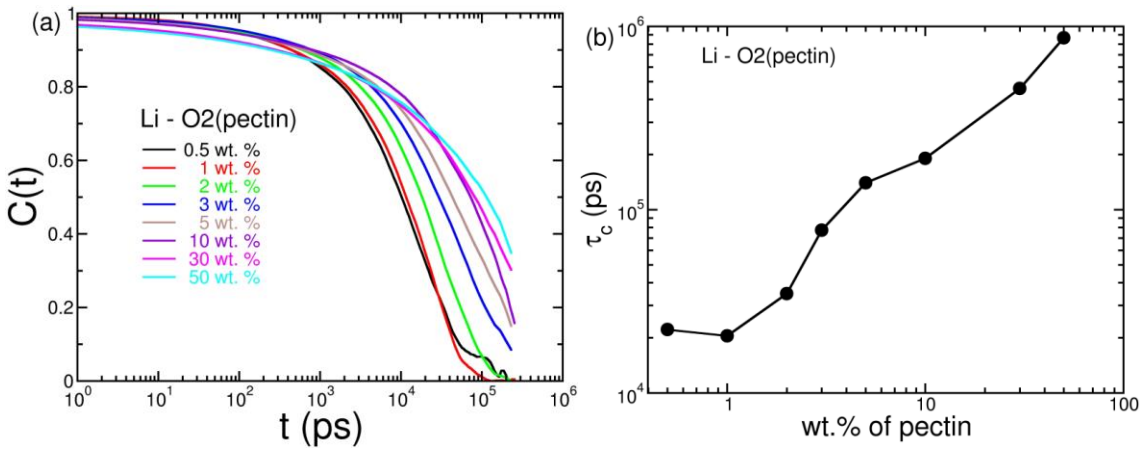

Figure S8.3: The Li-pectin correlation function and the corresponding residence time.

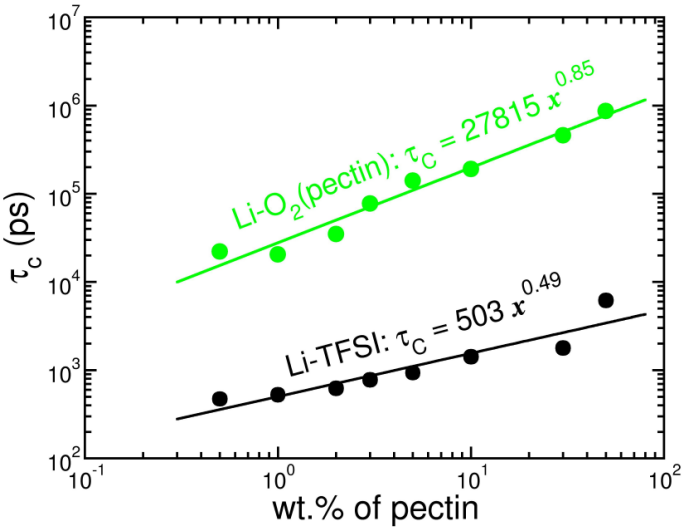

Figure S8.4: The residence time as a function of wt. % for Li-pectin and Li-TFSI fitted to equation $y = a_0 x^{a_1}$

S8: Pectin loading dependency of $\sigma_{NE}, \eta, P(0), P(1)$ and $P(2)$ and an intuitive objective function $f\left(\sigma_{NE}, P(0), P(1)\right) \sim \sigma_{NE} P^{a}(0)/P^{b}(1)$

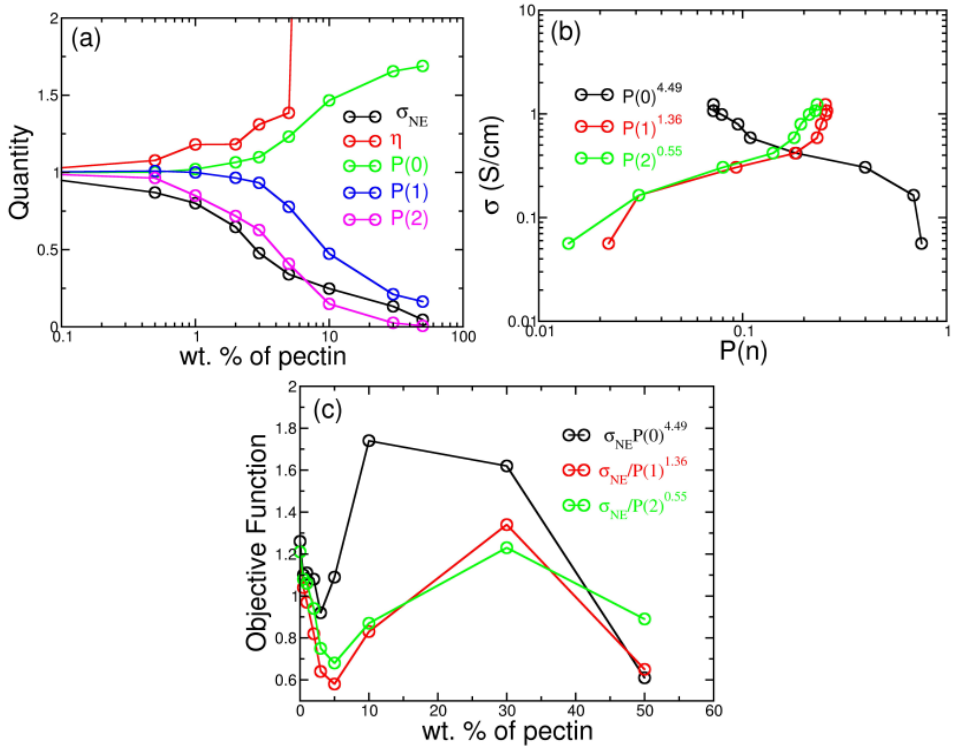

Figure S9: (a)The rate of change of $\sigma_{NE}, \eta, P(0), P(1)$ and $P(2)$ with the loading of pectin, (b) σ_{NE} as a function of ion association probability $P(n = 1,2,3)$, and (c) an intuitive objective function, $f\left(\sigma_{NE}, P(0), P(1)\right) \sim \sigma_{NE} P^{a}(0)/P^{b}(1)$

S9: Transference Number with wt. % of Pectin

To further understand how different ions contribute to conductivity, we have calculated the transference numbers for the Li+ and TFSI- ions with varying loadings of pectin. The transference numbers are defined from the self-diffusion coefficients of ions:

$$t_{Li} = \frac{D_{Li}}{D_{Li} + D_{TFSI}}$$

$$t_{TFSI} = \frac{D_{TFSI}}{D_{Li} + D_{TFSI}}$$

Here, D_{Li} and D_{TFSI} are diffusion coefficients, and t_{Li} and t_{TFSI} are the transference numbers of Li+ and TFSI- ions respectively. In **Figure S10**, we plotted the transference number with different wt. % of pectin loading. From quantitative transference number analysis, we find that the pectin-loaded EC-LiTFSI becomes a single ion conductor with wt. % of pectin loading as low as 10% as previously discussed in the diffusivity section. We see that our systems are excellent conductors for TFSI ions.

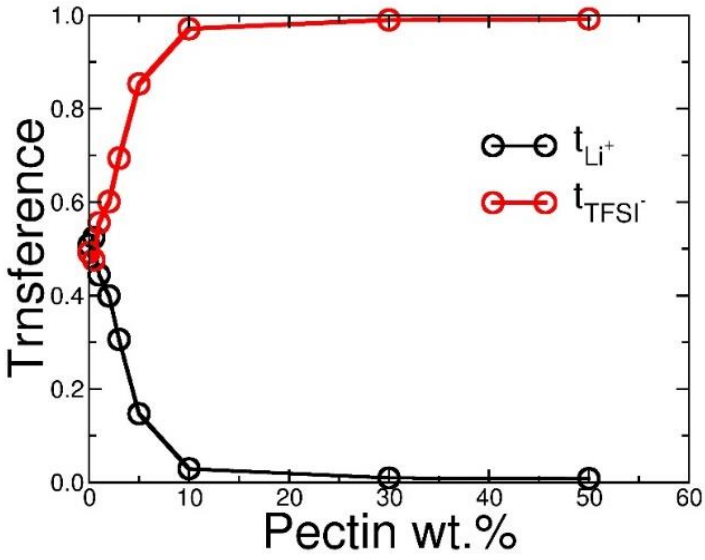

Figure S10: The calculated transference number of Li^+ and $TFSI^-$ ions for different wt.% of pectin-loaded systems from EMD simulations.

References:

[1] W. Humphrey, A. Dalke, and K. Schulten, *VMD: Visual Molecular Dynamics* (1996).
[2] K.N. Kirschner, A.B. Yongye, S.M. Tschampel, J. González-Outeiriño, C.R. Daniels, B.L. Foley, and R.J. Woods, J Comput Chem **29**, 622 (2008).
[3] Lindahl, Abraham, Hess, V. der Spoel, Lindahl, Abraham, Hess, and V. der Spoel, Zndo (2020).